Numerical simulation of cavitation in a Francis runner under different operating conditions

Agustí Mundet[1], Xavier Escaler[1*], Víctor H. Hidalgo[2]

[1]Department of Fluid Mechanics, Universitat Politècnica de Catalunya, Barcelona, Spain
[2]Departamento de Ingeniería Mecánica, Laboratorio de Informática - Mecánica, Escuela Politécnica Nacional, Quito, Ecuador

[*]xavier.escaler@upc.edu

ABSTRACT

The behavior of suction side leading edge cavitation on the runner blades of the GAMM Francis turbine has been investigated under different operating conditions at the best efficiency point (BEP) and at off-design operations. Steady state numerical simulations have been carried out with the Zwart-Gerber-Belamri (ZGB) two-phase model and with the Shear Stress Transport (SST) turbulence model available in ANSYS® CFX. The numerical model had been previously validated at BEP by comparing the cavity size and location, the pressure drop and the torque with experimental values obtained in a reduced scale model test utility. These results obtained at BEP have now been compared with analogous results calculated at different flow rates and heads. In particular, the runner flow has been computed at part load and at high load while keeping the nominal head. For that, the flow rate and the incidence angle of the inlet absolute velocity has been changed according to the corresponding guide vane opening angle. Furthermore, other operation conditions comprising higher and lower heads than the nominal one have also been considered, while keeping the angle of the inlet absolute velocity constant as if the guide vane position were the same for all the cases. The results show that the size of leading edge cavitation decreases significantly for operating conditions with lower flow rates and heads than the BEP. Meanwhile, similar cavitation developments are found for operating conditions with higher flow rates and heads than the BEP.

KEY WORDS: Inlet blade cavitation, Francis runner; GAMM turbine; off-design operation; Zwart cavitation model.

INTRODUCTION

Cavitation in hydraulic turbines is a very important hydrodynamic phenomenon that negatively affects their performance and may cause vibration, noise and erosion of the solid components. Therefore, cavitation has been an active topic for decades in the fields of hydrodynamics and turbomachinery, and its undying progress in simulation techniques and mechanism findings is expected. For a Francis turbine, it is evident that the runner design influences cavitation inception and development besides the operation conditions such as the machine setting level and the operating point [1]. The Francis turbine has the maximum efficiency up to 93-95% at best efficiency point (BEP), which declines at off-design conditions [2, 3]. The flow field also varies with operating conditions. Modern hydraulic turbines face the inconvenience associated with the variable demand on the energy market and the limitations of energy storage, leading to the need for flexibility in their operation. Consequently, hydraulic turbines are used for a wide range of operating regimes far from the operating point for which they have been designed. Moreover, radial-axial turbines (e.g. GAMM Francis turbine [4]) having a rotor with fixed pitch blades have a sharp drop in efficiency and severe pressure fluctuations at off-design operating regimes [5, 6]. Flow at off-design operations, such as part load and high load is not as stable as that of the BEP [7]. The operating conditions of Francis turbines are modified by changing the angular position of the guide vanes which adjusts the flow rate to meet the power required. The Francis turbine is designed to obtain the maximum hydraulic efficiency at one flow rate (i.e. BEP). However, turbine operation away from BEP develops instabilities and unsteady phenomena which reduce the overall efficiency of the turbine [2, 8]. To come closer to solving these problems, numerical and experimental research is still required to better understand the physics of the phenomenon [9].

The computational fluid dynamics (CFD) software ANSYS® CFX incorporates the unsymmetrical cavitation model proposed by Zwart-Gerber-Belamri (ZGB) [10], which is based on the interphase mass transfer, $\dot{m}$, derived from the Rayleight-Plesset equation. The ZGB model has already been used and validated several times in research for numerical prediction of sheet cavitation with fairly good results [11-13], and it has also been used for the numerical simulations presented in this study, along with the Shear Stress Transport (SST) turbulence model available in ANSYS® CFX. To evaluate the behavior of suction side leading edge cavitation on the runner blades of a Francis turbine, the GAMM Francis model geometry and performance [14-16] were taken as a study case.

EXPERIMENTAL DATA

The GAMM Francis turbine, with a specific speed $\nu = 0.5$, is characterized by a flow rate $Q = 0.376$ m³/s, a head $H = 5.957$ m, a rotating speed $\omega = 52.36$ rad/s, and a torque $T = 388$ Nm [16]. The hill diagram of the GAMM turbine is presented in Figure 1, represented by the discharge coefficient φ_{ref} and head coefficient ψ_{ref}, with regard to the IEC regulations [17]. The seven operation points studied in this work can be seen on the hill diagram, highlighted in red. The results obtained at BEP (Point 1, see Figure 1) have been compared with analogous results calculated at different flow rates and heads. Two different studies have been carried out, in the first one (highlighted in green, see Figure 1) the runner flow has been computed at part load (Point 4) and at high load (Point 5) while keeping the nominal head constant. In the second study (highlighted in orange, see Figure 1), four different operation conditions comprising higher and lower heads than the nominal one have been computed, while keeping the angle of the inlet absolute velocity, α, constant as if the guide vane position were the same for all the cases (Points 2, 3, 6 and 7).
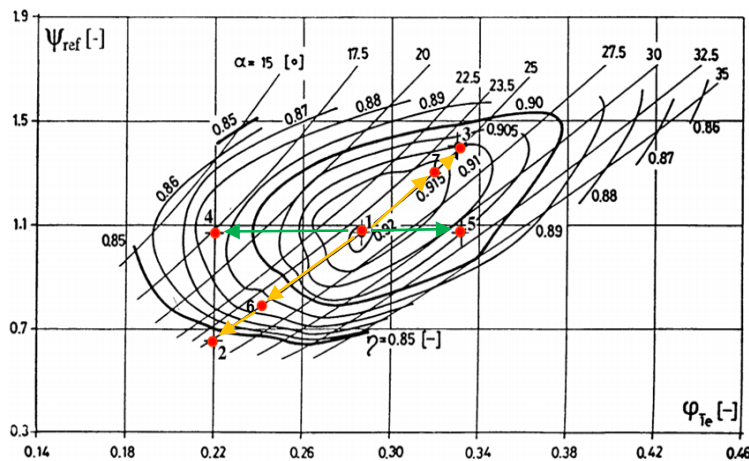

Figure 1 Hill diagram of the GAMM Francis turbine. Modified picture from the GAMM Proceedings [14].

Table 1 shows the corresponding dimensionless discharge and head coefficients, the angles of the inlet absolute velocity, and the efficiencies, η, of the seven operating conditions.

Table 1.Discharge and head coefficients, angles of inlet absolute velocity and efficiencies of each operating point [18].

Operating point	φ_{ref} (discharge coefficient)	ψ_{ref} (head coefficient)	α (guide vane angle)	η (efficiency)
P1-BEP	0.286	1.07	25.0º	0.920
P7	0.371	1.32	25.0º	0.915
P3	0.330	1.40	25.0º	0.910
P5	0.333	1.07	31.0º	0.905
P4	0.220	1.07	17.5º	0.885
P6	0.240	0.80	25.0º	0.880
P2	0.220	0.70	25.0º	0.850

The GAMM Francis turbine has a spiral casing which was designed to give a constant meridional velocity distribution, and in order to achieve well-defined inlet conditions, fillets were added on both sides of the distributor inlet. The distributor consists of 24 stay vanes and 24 guide vanes. The runner has 13 blades and an external diameter of 0.4 m, so the reference radius is $R_{ref} = 0.2$ m. The draft tube has a simple geometry without any inner pillar. The pressure and velocity distribution measurements of the BEP and the off-design conditions were made at the inlet of the distributor, at the inlet of the runner, just after the runner blades, at the inlet of the draft tube and at the outlet of

the draft tube. The measurements were carried out using a 6 mm diameter five-hole pressure probe, which provides the three components of the local flow components and the local static pressure [14, 19].

CAVITATION SIMULATIONS

Zwart-Gerber-Belamri (ZGB) Cavitation Model

To simulate the interphase mass transfer, $\dot{m}$, between the water and the vapor during vaporization and condensation the following Equations 1 and 2 are used respectively:
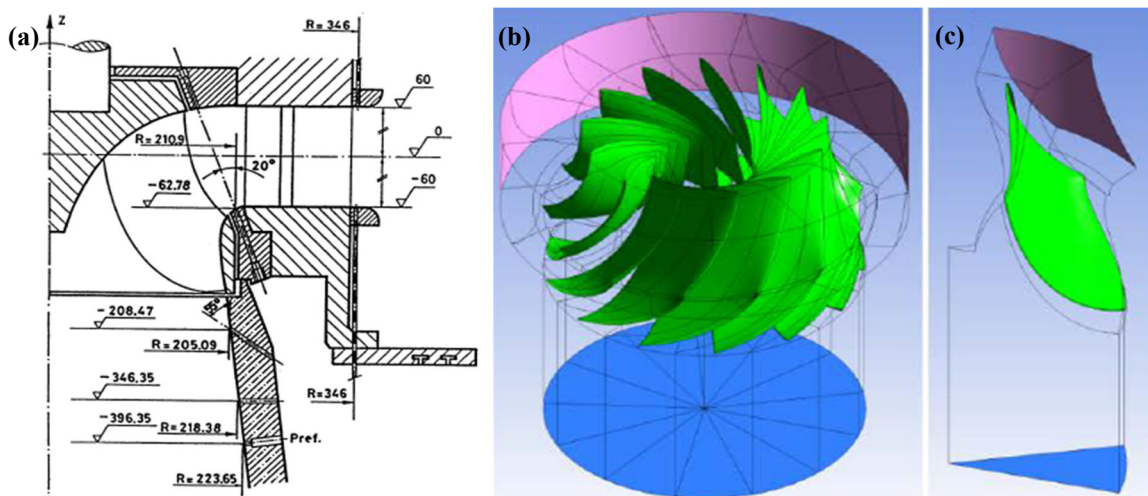
$$F_V \frac{3\alpha_{nuc}(1-\alpha_v)\rho_v}{R_B} \sqrt{\frac{2}{3}\frac{P_v-P}{\rho_l}} \ when \ P \leq P_v \tag{1}$$

$$F_c \frac{3\alpha_v\rho_v}{R_B} \sqrt{\frac{2}{3}\frac{P-P_v}{\rho_l}} \ when \ P > P_v \tag{2}$$

where R_B is the vapor bubble radius, α_{nuc} is the nucleation site volume fraction, α_v is the water vapor volume fraction, P_v is the saturated water vapor pressure, P is the local fluid pressure, and F_v and F_c are the empirical coefficients for vaporization and condensation, respectively. The default model constants in CFX® are $R_B = 10^{-6}$ m, $\alpha_{nuc} = 5 \cdot 10^{-4}$, $F_v = 50$ and $F_c = 0.01$.

Computational Domain

The turbine geometry in meridional plane is shown in Figure 2a. The stay vanes and the guide vanes were not considered in the computational domain. The runner fluid domain was bounded upstream by a cylindrical surface located in the middle of the distributor channel and extended downstream up to a circular surface in the draft tube channel as indicated in Figure 2b. To reduce computational effort and increase computation speed, a sector comprising only one inter-blade channel was created taking advantage of the rotational symmetry of the runner and the existence of 13 blades as shown in Figure 1c. Simulations were carried out using the Rotating Frames of Reference (RER) and the Shear Stress Transport (SST) turbulence model. The wall function method was used with the SST turbulence model to resolve the boundary layer with a relatively coarse mesh, which allowed to save CPU time and storage capacity. To validate such grid, a sensitivity analysis was first done with no cavitation model activated. The values simulated for head and torque showed a good agreement with the values from experimentation at BEP. As a result, the accurate mesh and the proper boundary conditions, necessary to predict the expected behavior, could be established in the model.

Figure 2 (a) Turbine cross section [14], (b) complete runner geometry, (c) single-channel computational domain.

Simulations

Firstly, the cavitation development was computed at BEP for different values of the outlet pressure P_{out} and of the

cavitation coefficient Sigma, σ, that was calculated with Equation 3 where g is the gravity:

$$\sigma = \frac{P_{out} - P_v}{\rho_l g H} \tag{3}$$

With decreasing σ, the typical torque rise was correctly simulated (see Figure 3a). The leading edge cavity was simulated and visualized with an isosurface of $\alpha_v = 0.5$. The location, size and shape of the simulated leading edge cavity at $\sigma = 0.15$ showed a good similarity with the visual observations in the reduced scale GAMM turbine model for $\sigma = 0.14$ [20], which was also in line with the works of Susan-Resiga *et al.* [13, 14].
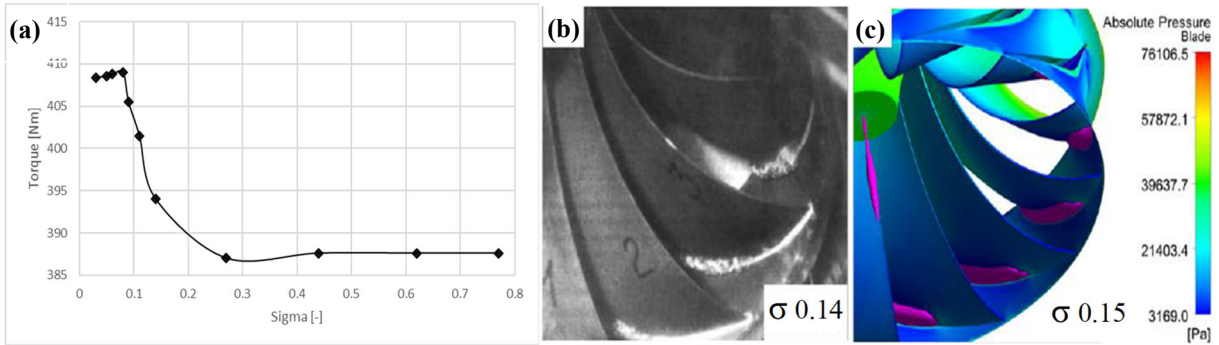

Figure 3: (a) Simulated runner torque evolution with σ, (b) photography of the inlet edge cavitation in the GAMM Francis turbine model at BEP for $\sigma = 0.14$ [20], (c) contours of absolute pressure and isosurface of $\alpha_v = 0.5$ for $\sigma = 0.15$.

To study at which extent the size and shape of leading edge cavitation changes as a result of the turbine off-design operation, two studies were carried out.

BEP (nominal flow rate): $\varphi_{ref} = 0.286$, $\psi_{ref} = 1.07$, $\alpha = 25^\circ$, $\eta = 0.920$.
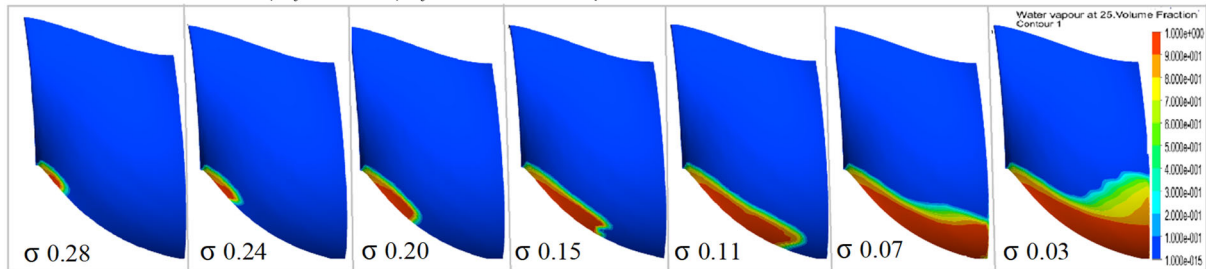
Point 4 (low flow rate): $\varphi_{ref} = 0.22$, $\psi_{ref} = 1.07$, $\alpha = 17.5^\circ$, $\eta = 0.885$.
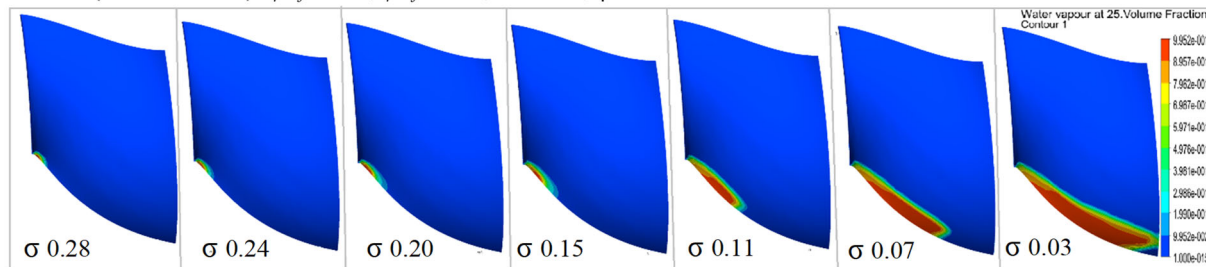
Point 5 (high flow rate): $\varphi_{ref} = 0.33$, $\psi_{ref} = 1.07$, $\alpha = 31^\circ$, $\eta = 0.905$
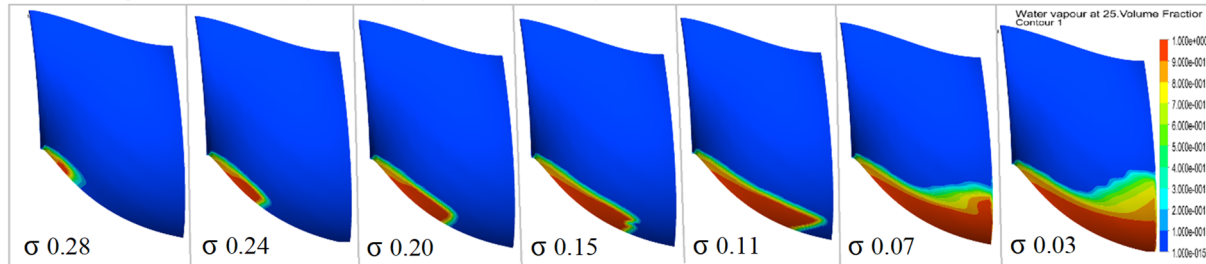

Figure 4: α_v of Points 5, 4 and BEP for different values of σ, keeping constant nominal head $\psi_{ref} = 1.07$.

Firstly, the runner flow was computed at part load with a flow rate below the design flow rate (Point 4) and at high load with a flow rate above the design flow rate (Point 5) while keeping the nominal head constant at $\psi_{ref} = 1.07$. In Figure 4, the leading edge cavity has been visualized with the α_v plotted on the suction side of the blade. It can be clearly observed how cavitation develops as σ decreases. The size of the contact region of the cavitation with the blade suction side is similar between the BEP and the P5 at high flow rate. On the contrary, the P4 at low flow rate shows significantly smaller cavities than the BEP for the same σ.

Secondly, four different operation conditions (Points 2, 3, 6 and 7) comprising higher and lower heads than the nominal one, while keeping $\alpha = 25^{o}$ as if the guide vane position were the same for all the cases, were computed. In Figure 5, the predicted leading edge cavity has been visualized with the α_v plotted on the suction side of the blade. It can be clearly observed how cavitation develops as σ decreases. However, for P2 with the lowest head and flow rate and for P6 closer to it but with slightly higher flow and head the cavitation only appears for very small σ values below 0.1. On the contrary, for P7 and P8, all the flow conditions present a significant leading edge cavity on the blade for any σ value up to 0.23.
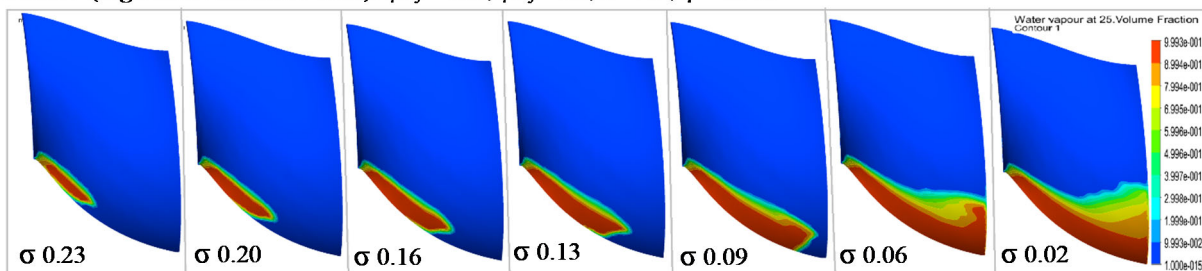
Point 2 (low head and flow rate): $\varphi_{ref} = 0.22$, $\psi_{ref} = 0.7$, $\alpha = 25^{o}$, $\eta = 0.850$.
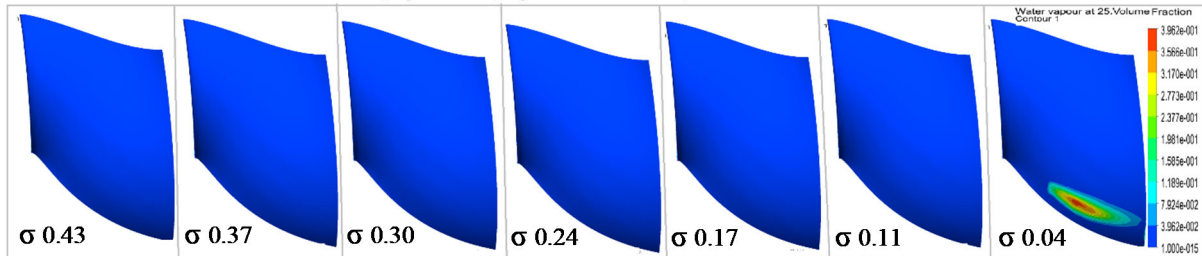
Point 6 (low head and flow rate): $\varphi_{ref} = 0.24$, $\psi_{ref} = 0.8$, $\alpha = 25^{o}$, $\eta = 0.885$.
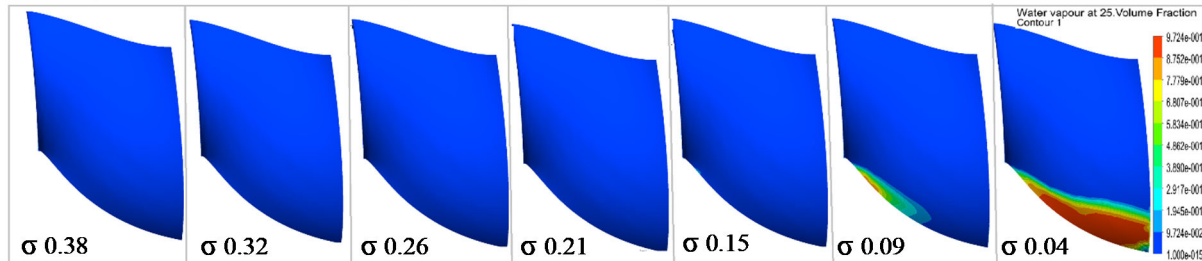
Point 7 (high head and flow rate): $\varphi_{ref} = 0.37$, $\psi_{ref} = 1.3$, $\alpha = 25^{o}$, $\eta = 0.915$.

Point 3 (high head and flow rate): $\varphi_{ref} = 0.33$, $\psi_{ref} = 1.4$, $\alpha = 25^{o}$, $\eta = 0.910$.
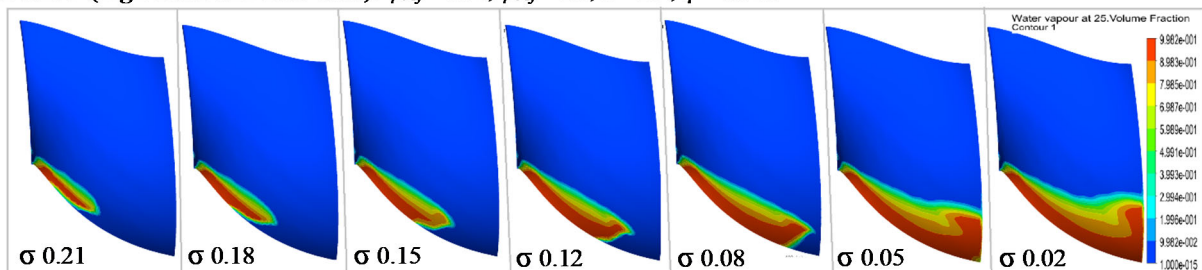

Figure 5: α_v of Points 2, 3, 6 and 7 for different values of σ, with a constant $\alpha = 25^{o}$.

The general impression from the previous plots is that for all the operating conditions simulated at part load a lower extent of leading edge cavitation develops on the blade. Under such conditions (Points 2, 4 and 6), cavitation inception takes place for lower σ values than for the rest of cases (Points 1, 3, 5, 7). To confirm such conclusion, the entire runner showing the 3D shape and location of the predicted cavitation has been plotted in Figure 6 for all operating points at similar σ values around 0.15. It must be noted that for points 1, 3 and 5 a draft tube vortex rope is also visualized because its core also suffers cavitation.
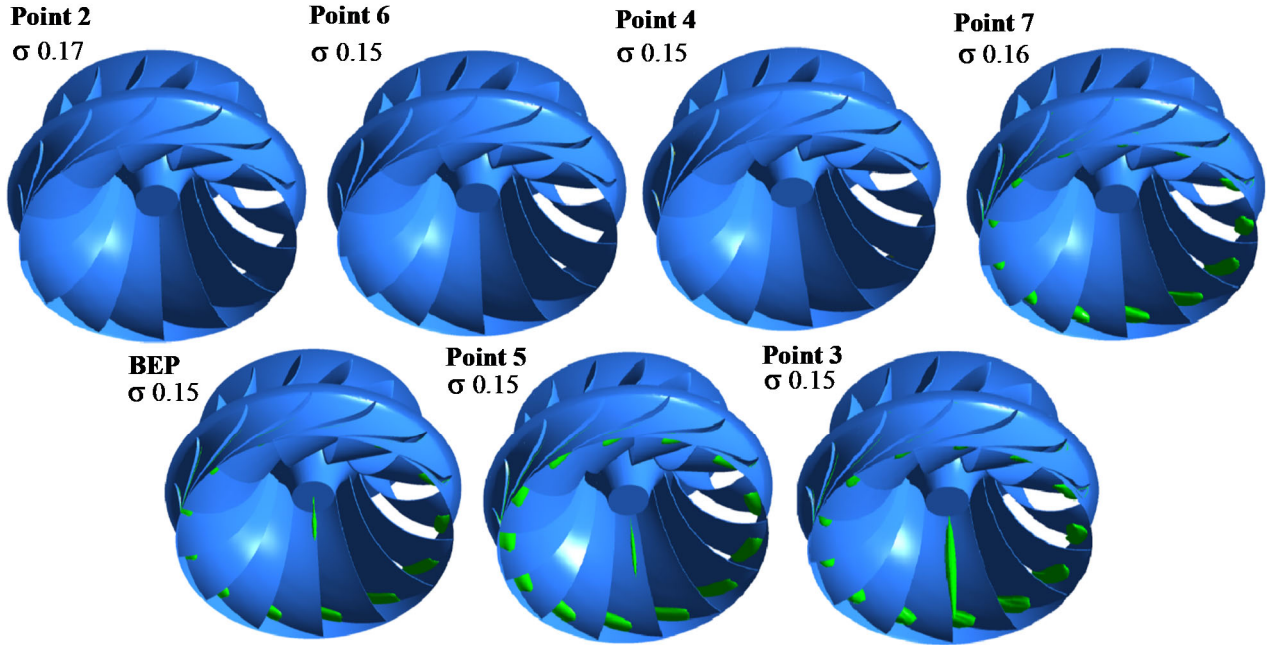

Figure 6 Location and shape of cavitation for each operating point at σ around 0.15, shown with a green isosurface of $\alpha_v = 0.5$.

In order to quantify such differences, the area on the suction side of the blade with $\alpha_v \geq 0.5$ has been measured and it has been plotted in Figure 7 as a function of σ for all the operating conditions. The plots shown in Figure 7 demonstrate that the cavitation development is similar for all the points comprising the BEP and those with higher flow rates and heads than the nominal one, and that for lower flow rates and heads the cavitation development is significantly reduced. The different behavior between part load and high load conditions could be related to the significantly lower efficiency of the part load points. In particular, P2, P4 and P6 have $\eta \leq 0.885$ but P1, P3, P5 and P7 have $\eta \geq 0.905$ as it can be checked from the values presented in Table 1.

The similar cavitation development observed by all the operating points at nominal condition and at higher flow rates and heads than the BEP has permitted to infer a mathematical expression of the total cavitation area on the blade as a function of σ. The study of the numerical results has indicated that an exponential law gives the best fit to the data points with a coefficient of determination, R^2, of 0.98. The obtained Equation (4) giving a predicted area on the blade with $\alpha_v \geq 0.5$ is the following one:

$$Cavitation\ Area\ on\ blade\ (\alpha_v \geq 0.5) = 0.01e^{-11.3\sigma} \tag{4}$$

The predicted values given by Equation (4) have been plotted together with the simulated results for BEP and Points 3, 5 and 7 in Figure 8 showing a very good agreement.
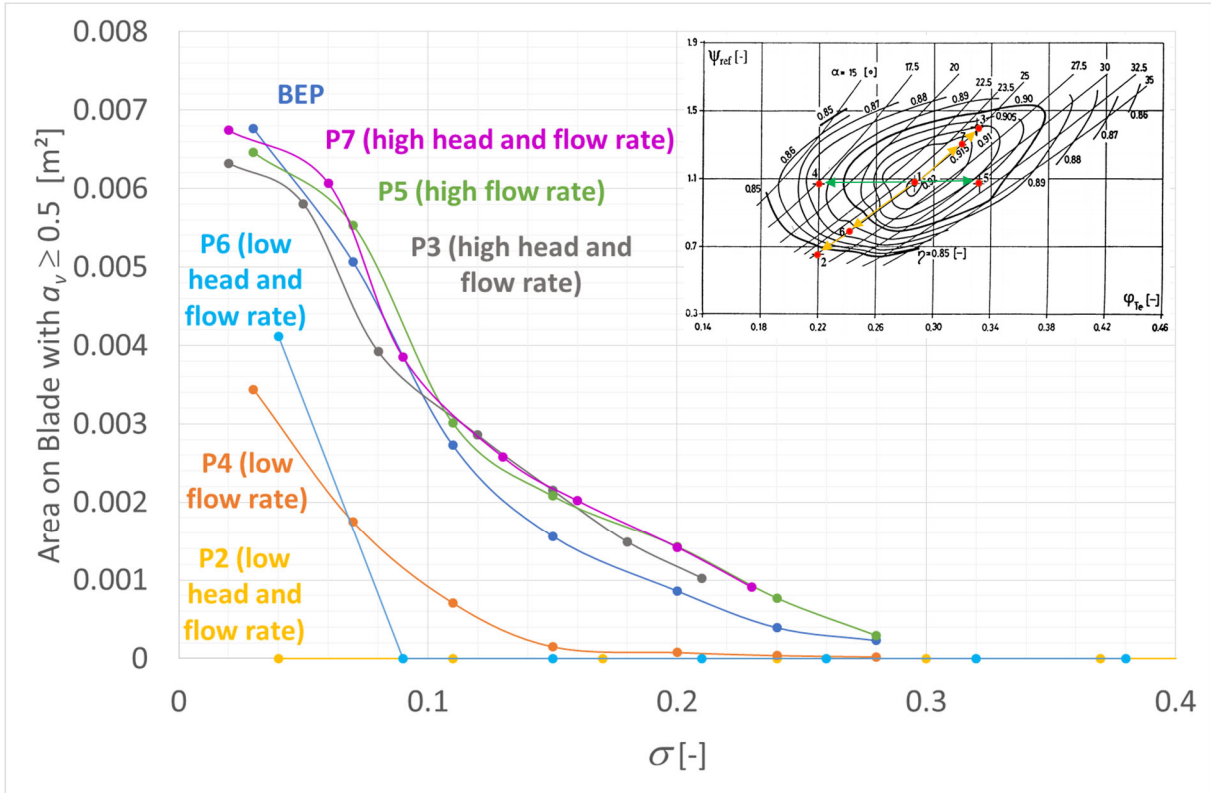
Figure 7: Evolution of the area on blade covered by cavitation with $\alpha_v \geq 0.5$ as σ decreases for all the operating points.
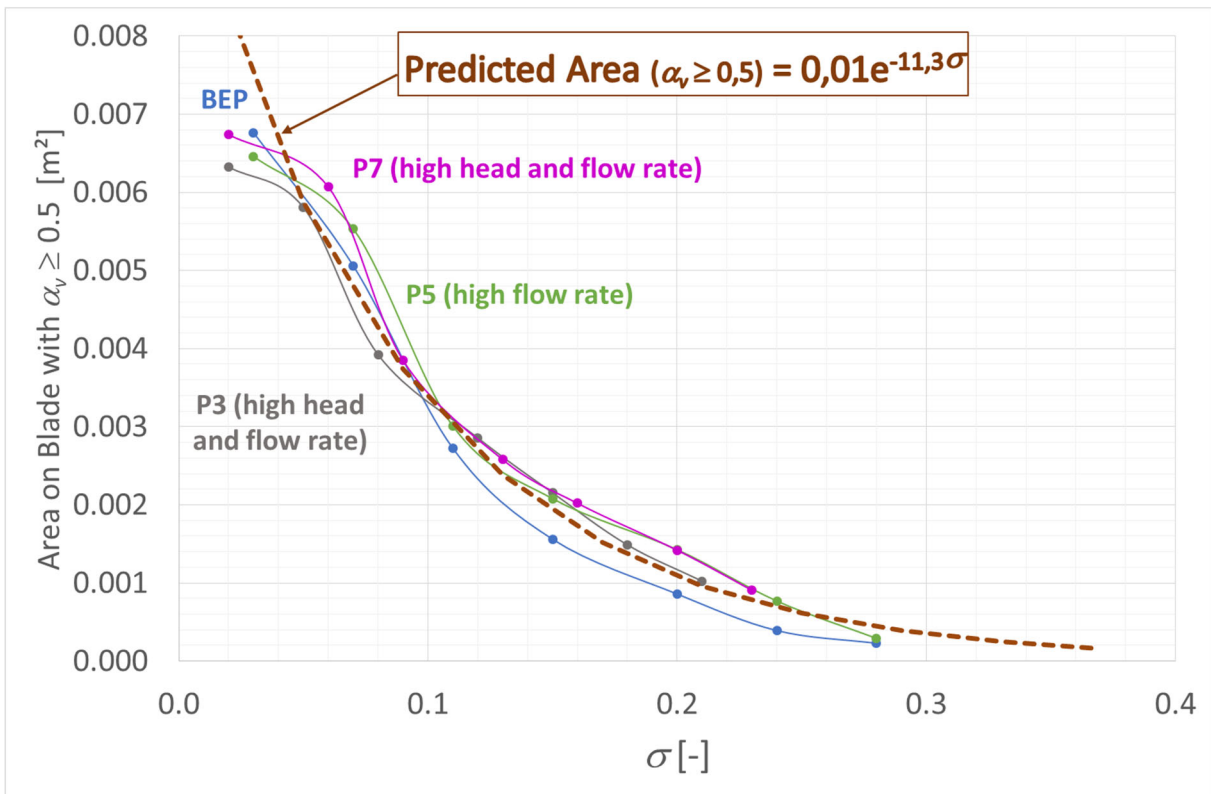

Figure 8: Evolution of the area on blade covered by cavitation with $\alpha_v \geq 0.5$ as σ decreases calculated with Equation (4) and simulated values at BEP and at higher flow rates and heads.

CONCLUSIONS

Inlet cavitation on the suction side of the runner blades of the GAMM Francis turbine has been simulated at BEP and at various off-design operating conditions both at part loads and high loads. The ZGB cavitation model and the SST turbulence model have been used to carry out the steady state calculations. The numerical model has been proved to give reliable results at BEP by comparison with flow visualizations obtained from reduced scale experimental tests. The simulations show that, keeping the same σ, the size of the leading edge cavitation decreases significantly for part load operating conditions (lower flow rates and heads than the BEP), but it is similar for high load operating conditions (higher flow rates and heads than the BEP). As a result, a mathematical expression to predict the area of the blade with cavitation as a function of σ has been obtained for BEP and off-design operation conditions at high loads.

REFERENCES

[1] Luo X., Ji B., and Tsujimoto Y. (2016) *A review of cavitation in hydraulic machinery.* Journal of Hydrodynamics, Ser. B, Volume 28, Issue 3, Pages 335-358.

[2] Goyal R., and Gandhi B. (2018) *Review of hydrodynamics instabilities in Francis turbine during off-design and transient operations.* Renewable Energy, Volume 116, Part A, Pages 697-709.

[3] Trivedi C. (2014) *Experimental and numerical investigations on steady state and transient characteristics of a high head Francis turbine.* P.hD. thesis, Indian Institute of Technology, Roorkee, India.

[4] P. Henry, M. Hussain-Khan, (1997), *Francis Turbine Runner: Blade Design.* In Radha Krishna H.C. (ed.) Hydraulic Design of Hydraulic Machinery, Avebury Publishing House.

[5] Ciocan T., Susan-Resiga R., and Muntean, S. (2006). *Analysis of the swirling flow at GAMM Francis runner outlet for different values of the discharge.* Proc. of the XXXIIIrd Caius-Iacob Conference On Fluid Mechanics and Its Technical Applications, Bucharest, Romania, 2011, pp. 33–41.

[6] Escudier M. (1987) *Confined vortices in flow machinery*, Annual Review of Fluid Mechanics 19 27–52.

[7] Iliescu M., Ciocan G., and Avellan F. (2008) *Analysis of the cavitating draft tube vortex in Francis turbine using particle image velocimetry measurements in two-phase flow,* J. Fluids Eng. 130 021105.

[8] Trivedi C., Cervantes M., Bhupendra G., and Dahlhaug O. (2013) *Experimental, Numerical, Studies for high head Francis turbine at several operating points.* ASME, J. Fluids Eng. 135 (11) 111102.

[9] Ji, B., Long, Y., Long, X., Qian, Z., and Zhou, J. (2017) *Large eddy simulation of turbulent attached cavitating flow with special emphasis on large scale structures of the hydrofoil wake and turbulence-cavitation interactions.* Journal of Hydrodynamics, Ser. B, 29(1):27-39.

[10] Zwart, P., Gerber, A. and Belamri, T. (2004) *A Two-Phase Flow Model for Predicting Cavitation Dynamics.* Proceedings of the ICMF 2004 Int. Conf. on Multiphase Flow, Yokohama, Japan.

[11] Hidalgo, V., Luo, X. W., Escaler, X., Bin, J. I. and Aguinaga, A. (2015). *Implicit large eddy simulation of unsteady cloud cavitation around a plane-convex hydrofoil.* Journal of Hydrodynamics, Ser. B, 27(6), 815-823.

[12] Morgut, M., Nobile, E. and Biluš, I. (2011) *Comparison of mass transfer models for the numerical prediction of sheet cavitation around a hydrofoil.* International Journal of Multiphase Flow, 37(6):620–626.

[13] Morgut, M., Jošt, D., Škerlavaj, A., Nobile, E. and Contento, G. (2017) *Numerical Predictions of Cavitating Flow Around a Marine Propeller and Kaplan Turbine Runner with Calibrated Cavitation Models.* Strojniški vestnik – Journal of Mechanical Engineering. Article in Press.

[14] Avellan, F., Dupont, P., Farhat, M., Gindroz, B., Henry, P., Hussain, M., Parkinson, E. and Santal, O. (1990) *Flow Survey and blade pressure measurements in a Francis turbine model.* Proceedings of 15th IAHR Symposium on modern technology in hydraulic energy production, September 1990, Belgrade, vol. 2, Session I, Paper 14, 14 pages.

[15] Avellan F., Dupont P., Farhat M., Gindroz B., Henry P. and Hussain M. (1993) *Experimental flow study of the GAMM turbine model.* Proceedings of the GAMM Workshop "3D-computation of incompressible internal flow" Ed. Sottas G. and Ryhming I.L., NNFM 39, Vieweg Verlag, Braunschweig, pp. 33-53.

[16] Sottas G., Ryhming I.L., (eds.), (1993) "3D – Computation of Incompressible Internal Flows", *Proceedings of the GAMM Workshop, Notes Numerical Fluid Mechanics* (NNFM) 39, Vieweg Verlag, Braunschweig.

[17] International Electrotechnical Commision, (1999), *Hydraulic Turbines, Storage Pumps and Pump - Turbines — Model Acceptance Tests*, International Standard IEC 60193, 2nd ed.

[18] Gros L., Kueny J.L., Avellan F., and Bellet L. (1998) *Numerical flow analysis of the GAMM turbine at nominal and off-design operating conditions.* In Proceedings of the XIX IAHR Symposium, Hydraulic Machinery and Cavitation, pages 121–128.

[19] Nilsson H., Davidson L., (2001) *A validation of parallel multiblock CFD against the GAMM Francis water turbine runner at best efficiency and off-design operating conditions.* Int.rep.01/02, Dept. of Thermo and Fluid Dynamics, Chalmers University of Technology, Göteborg, Sweden.

[20] Liu, H-l., Wang, J., Wang, Y., Zhang, H. and Huang, H. (2014). *Influence of the empirical coefficients of cavitation model on predicting cavitating flow in the centrifugal pump.* International Journal of Naval Architecture and Ocean Engineering, 6(1):119–131.